OPEN

Platonic Scattering Cancellation for Bending Waves in a Thin Plate

M. Farhat[1], P.-Y. Chen[2], H. Bağcı[1], S. Enoch[3], S. Guenneau[3] & A. Alù[2]

[1]Division of Computer, Electrical, and Mathematical Sciences and Engineering, King Abdullah University of Science and Technology (KAUST), Thuwal 23955-6900, Saudi Arabia, [2]Department of Electrical and Computer Engineering, The University of Texas at Austin, Austin, TX, 78712, USA, [3]Aix-Marseille Université, CNRS, Centrale Marseille, Institut Fresnel, UMR 7249, 13013 Marseille, France.

We propose an ultra-thin elastic cloak to control the scattering of bending waves in isotropic heterogeneous thin plates. The cloak design makes use of the scattering cancellation technique applied, for the first time, to the biharmonic operator describing the propagation of bending waves in thin plates. We first analyze scattering from hard and soft cylindrical objects in the quasistatic limit, then we prove that the scattering of bending waves from an object in the near and far-field regions can be suppressed significantly by covering it with a suitably designed coating. Beyond camouflaging, these findings may have potential applications in protection of buildings from earthquakes and isolating structures from vibrations in the motor vehicle industry.

I n the past few years, metamaterials have become an attractive research focus for physicists and engineers due to their ability to control electromagnetic, acoustic, and elastic waves in ways that cannot be achieved using "regular" materials. Consequently, exciting applications of metamaterials ranging from sub-wavelength imaging to cloaking have been reported[1–22]. Soon after the advent of negative refraction and sub-wavelength imaging[1], it has been shown that dielectric or conducting objects could be made "invisible" to electromagnetic waves by coating them with plasmonic materials[2,3]. A promising route to electromagnetic invisibility relies on the scattering cancellation phenomenon, where the fields scattered from a coating with negative (local) polarizability are specifically designed to cancel the fields scattered from the object[2,4–7]. The scattering cancellation technique has been proven relatively robust to changes in the design parameters, geometry, losses, and frequency of operation[8,9]. It has also been used to make electrodes or metal films transparent to THz[10] or GHz[11] radiation. Experimental evidence of such invisibility devices has recently been demonstrated in the microwave regime[12–14]. An alternative route to designing invisibility devices makes use of coordinate transformations[15,16] to mold the wave flow in desired manners[17–22]. It should also be mentioned here that with their possible applications in stealth technology, noninvasive probing, and sensing, electromagnetic invisibility cloaks open promising avenues for new technologies in medicine, defense, and telecommunications[23,24].

Cloaking ideas and designs for acoustic waves have also been developed. The possibility of two-dimensional acoustic cloaking for pressure waves in transversely anisotropic fluids has recently been shown[25]. Subsequent investigation of this cloaking idea for concentric layers of solid lattices behaving as artificially anisotropic fluids in the homogenization limit has been provided[26]. Following a similar approach, a micro-structured metallic structure has been designed as a cloak for surface liquid waves; the design has been validated experimentally around 10 Hz[27]. Additionally, three-dimensional acoustic cloaking for pressure waves in fluids has been envisaged; this cloak makes use of the fact that the scalar wave equation retains its form under geometric transforms[28,29]. Like in electromagnetic cloaking, the scattering cancellation technique offers an alternative path towards acoustic cloaking[30–32]. However, cloaking fully coupled pressure and shear elastodynamic waves in solids is a more elusive task, since the Navier-Stoke's equations do not retain their form under geometric transforms[33,34]. Although the theoretical foundation of these cloaking effects is well established[35,36], the inherent requirement of singular bulk metamaterial properties that can hardly be met in practice still hinders the practicality of cloaking devices[37,38].

In this Report, a biharmonic wave equation with appropriate boundary conditions, which describes the propagation of bending waves, is derived from the generalized elasticity theory[39,40] and is used in designing a cloak that operates in thin plates. The idea behind the cloak design is to choose a coating material with density ρ_c satisfying $\rho_c < \rho_0$ or $\rho_c < 0$ and to conceal an object with density $\rho_s > \rho_0$. Here, ρ_0 represents the density of the surrounding medium.

The parameters of the cloak are deduced using the scattering cancellation technique applied to a *platonic* metamaterial coating[2]. Note that the term "platonic" was coined by McPhedran in reference to thin plates while investigating wave propagation in complex thin plate elastic artificial materials[41–43]. Recent advances in the field of high frequency homogenization in platonics provide a theoretical foundation for understanding frequency dependent effective mass density taking negative or less than unity values[44].

We then analyze the response of the platonic cloak concealing a cylindrical obstacle in the presence of a plane wave elastic excitation (harmonic vibration of the plate in the vertical z-direction). It is assumed that the out-of-plane dimension of the obstacle is negligible compared to its in-plane dimensions[41,42]. We show that in the quasi-static limit, i.e. for $k_0 a_s \ll 1$, where k_0 is the bending wavenumber in the surrounding medium and a_s is the in-plane dimension of the scatterer, the scattering is dominated by the zeroth-order multipole, unlike in the electrodynamics case where the first significant order is the dipolar one. This is not the only fundamental difference between electrodynamic/acoustic and elastic wave scattering phenomena: the fourth order biharmonic partial differential equation, which typically describes the propagation of bending waves in ultra-thin plates, is not equivalent to the vector/scalar wave equations that describe electromagnetic or acoustic wave propagation. For instance note that propagating and evanescent waves coexist even in homogeneous thin plates. Consequently, one can anticipate that a new cloaking method and new relevant physics are introduced following this route.

Results

It has been recently shown that the elasticity equations are not invariant under coordinate transformations[33]. Indeed, equations describing the propagation of elastodynamic waves under a time harmonic dependence $e^{-i\omega t}$ read (in a weak sense)

$$\nabla \cdot \mathbf{C} : \nabla \mathbf{u} + \rho_0 \omega^2 \mathbf{u} = \mathbf{0}. \quad (1)$$

Here, ρ_0 is the (scalar) density of an isotropic heterogeneous elastic medium, $\mathbf{C}$ is the rank-four symmetric elasticity tensor (which has up to 3^4 entries even for thin plates), ω is the wave angular frequency, and $\mathbf{u}$ is the associated three-component vector displacement field. In most practical applications, the lateral dimension is significantly larger than the plate thickness making the Kirchhoff assumption for thin plates applicable[39,40]. Under this assumption, shear deformation and rotary inertia are negligible. For such a structure, Eq. (1) reduces to the scalar fourth order biharmonic equation

$$\nabla \cdot \left\{ E(r)^{1/2} \nabla \left[[\rho(r)/\rho_0]^{-1/2} \nabla \cdot \left(E(r)^{1/2} \nabla U(r,\theta) \right) \right] \right\} - \quad (2)$$
$$[\rho(r)/\rho_0]^{1/2} k_0^4 U(r,\theta) = 0,$$

where $U(r, \theta)$ is the displacement in the vertical z-direction (assuming a cylindrical coordinate system due to the symmetry of the structure), $E(r)$ is the relative Young modulus, $\rho(r)$ is the density, $k_0^4 = \omega^2 \rho_0 h/D_0$, D_0, and ρ_0 are the bending wavenumber (to the power four), rigidity and density in the thin plate, respectively, and h is the plate thickness. Consider the structure shown in the inset of the Fig. 1. An object of radius a_s is coated with a shell of outer radius a_c. For $r < a_s$ (inside the object), $\rho(r) = \rho_s$ and the bending wavenumber is k_s. For $a_s < r < a_c$ (inside the shell), $\rho(r) = \rho_c$ and the bending wave number is k_c. Object, shell, and thin plate all have the same rigidity $D(r) = D_0$, same relative Young modulus $E(r) = 1$, and same Poisson's ratio $v(r) = v_0$. Without loss of generality, we assume that this structure is illuminated by a plane wave propagating in the x-direction. The displacement field of the incident plane wave is expressed as $U^{inc}(r,\theta) = e^{ik_0 r \cos\theta}$, equivalently it can be expanded as

$U^{inc}(r,\theta) = \sum_{n=0}^{\infty} \varepsilon_n i^n J_n(k_0 r) \cos n\theta$, where the coefficients $\varepsilon_0 = 1$ and $\varepsilon_n = 2, n \geq 2$. The scattered field, $U^{sca}(r, \theta)$, must be finite at $r = 0$ and it satisfies the radiation condition at $r \to \infty$. Thus, it is expressed as
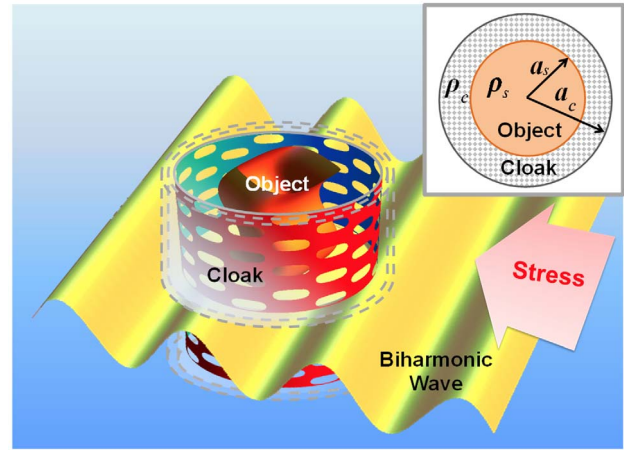

Figure 1 | Geometry under investigation: An object at the center of a thin elastic plate lies on the trajectory of a planar bending wave, incident from right to left in presence of a cylindrical shell that may act as a platonic cloak. Inset shows a top view of the cloak and object.

$$U^{sca}(r,\theta) = \sum_{n=0}^{\infty} \varepsilon_n i^n [A_n H_n^{(1)}(k_0 r) + B_n K_n(k_0 r)] \cos n\theta, \; r > a_c. \quad (3)$$

Similarly, fields inside the shell and the object are expressed as

$$U^{cloak}(r,\theta) = \sum_{n=0}^{\infty} \varepsilon_n i^n [C_n Y_n(k_c r) + D_n K_n(k_c r) + E_n J_n(k_c r)$$
$$+ F_n I_n(k_c r)] \cos n\theta, \; a_s < r < a_c, \quad (4)$$

$$U^{int}(r,\theta) = \sum_{n=0}^{\infty} \varepsilon_n i^n [G_n J_n(k_s r) + H_n I_n(k_s r)] \cos n\theta, \; r < a_s,$$

respectively. Here, $H_n^{(1)}(.)$, $J_n(.)$ and $I_n(.)$, and $Y_n(.)$ and $K_n(.)$ are cylindrical Hankel functions of the first kind, Bessel and modified Bessel functions, and Bessel and modified Bessel functions of the second kind, respectively. To solve for the coefficients in the above equations, continuity of the field U, its derivative in radial direction $\partial U/\partial r$, the bending momentum M_r, and the radial component of the generalized Kirchhoff stress V_r is enforced at the boundaries at $r = a_s$ and $r = a_c$, for each azimuthal order n (see supplemental materials[45] for explicit expressions of the bending momentum and the generalized Kirchhoff stress in cylindrical coordinates). This yields a matrix system of equations in scattering unknown coefficients A_n and B_n. The far-field scattering amplitude (or differential scattering cross-section) $f(\theta) = \sqrt{2r} e^{-i(k_0 r - \pi/4)} \lim_{r\to\infty} U^{sca}(r,\theta)$ is a measure of the cloaked object's visibility in direction θ[46]. The total scattering cross-section, σ^{sca}, is the integral of $f(\theta)$ over all angles, i.e. $\sigma^{sca} = 1/2 \int_0^{2\pi} d\theta |f(\theta)|^2$. It may thus be expressed as

$$\sigma^{sca} = \frac{4}{k_0} \sum_{n=0}^{\infty} \varepsilon_n |A_n|^2. \quad (5)$$

Note that coefficients B_n are absent in Eq. (5) since the modified Bessel functions $K_n(k_0 r)$ have no contribution to the scattered field as $r \to \infty$. Generally speaking, the possibility for an observer to detect the object in the far-field is determined by the value of σ^{sca}. As a result, minimizing or completely canceling σ^{sca} would lead to the undetectability (invisibility) of the object in the far-field, independent of the observer's position. This can be achieved by canceling the coefficients $A_n = \tilde{A}_n/d_n$ that significantly contribute to the scattering. Here, $\tilde{A}_n$ is given by the determinant:

$$\begin{vmatrix}
-J_n(k_0a_c) & K_n(k_0a_c) & -Y_n(k_ca_c) & -K_n(k_ca_c) & -J_n(k_ca_c) & -I_n(k_ca_c) & 0 & 0 \\
0 & 0 & Y_n(k_ca_s) & K_n(k_ca_s) & J_n(k_ca_s) & I_n(k_ca_s) & -J_n(k_sa_s) & -I_n(k_sa_s) \\
k_0J'_n(k_0a_c) & k_0K'_n(k_0a_c) & -k_cY'_n(k_ca_c) & -k_cK'_n(k_ca_c) & -k_cJ'_n(k_ca_c) & -k_cI'_n(k_ca_c) & 0 & 0 \\
0 & 0 & k_cY'_n(k_ca_s) & k_cK'_n(k_ca_s) & k_cJ'_n(k_ca_s) & k_cI'_n(k_ca_s) & -kJ'_n(k_sa_s) & -kI'_n(k_sa_s) \\
S_{J_n}(k_0a_c) & S_{K_n}(k_0a_c) & -S_{Y_n}(k_ca_c) & -S_{K_n}(k_ca_c) & S_{J_n}(k_ca_c) & S_{I_n}(k_ca_c) & 0 & 0 \\
0 & 0 & S_{Y_n}(k_ca_s) & S_{K_n}(k_ca_s) & S_{J_n}(k_ca_s) & S_{I_n}(k_ca_s) & -S_{J_n}(k_sa_s) & S_{I_n}(k_sa_s) \\
T_{J_n}(k_0a_c) & T_{K_n}(k_0a_c) & -T_{Y_n}(k_ca_c) & -T_{K_n}(k_ca_c) & T_{J_n}(k_ca_c) & T_{I_n}(k_ca_c) & 0 & 0 \\
0 & 0 & T_{Y_n}(k_ca_s) & T_{K_n}(k_ca_s) & T_{J_n}(k_ca_s) & T_{I_n}(k_ca_s) & -T_{J_n}(k_sa_s) & T_{I_n}(k_sa_s)
\end{vmatrix} \quad (6)$$

where

$$S_{Z_n}(k_ir) = D_0[n^2(1-v_0)(k_ir)^2]Z_n(k_ir) - D_0(1-v_0)\,k_ir\,Z'_n(k_ir),$$
$$T_{Z_n}(k_ir) = D_0[n^2(1-v_0)]Z_n(k_ir) - D_0[n^2(1-v_0)(k_ir)^2]\,k_ir\,Z'_n(k_ir), \quad (7)$$

where $k_i \in \{k_s, k_c, k_0\}$ and $Z_n(.) \in \{J_n(.), Y_n(.), H_n^{(1)}(.), K_n(.), I_n(.)\}$. Upper and lower signs in Eq. (7) should be selected for $Z_n(.) \in \{J_n(.), Y_n(.), H_n^{(1)}(.)\}$ and $Z_n(.) \in \{K_n(.), I_n(.)\}$, respectively. The expression of d_n could be obtained from Eq. (6) by replacing $J_n(.)$ by $H_n(.)$ in the first column (see supplemental materials[45]). Given the general complexity of this expression, it is instructive to analyze the low frequency limit corresponding to elastically small obstacles and shells, i.e. $k_ca_c \ll 1$, $k_sa_s \ll 1$, $k_0a_c \ll 1$, and $k_0a_s \ll 1$. Note that with the parameters in our study, it is sufficient to impose only $k_0a_s \ll 1$ and $k_0a_c \ll 1$. Under this assumption, σ^{sca} in Eq. (5) is dominated by the monopole term A_0:

$$\sigma^{sca} \approx \frac{4}{k_0}|A_0|^2 \approx \frac{\pi^2(k_0a_c)^4}{16k_0}[\rho_c - \rho_0 + \gamma^2(\rho_s - \rho_c)]^2, \gamma = a_s/a_c. \quad (8)$$

Note that here, terms scaling with $(k_0a_c)^m$, $m \geq 3$, in expressions of A_n, $n \geq 0$, are safely assumed to be zero for $k_0a_c \ll 1$. It is clear from Eq. (8) that σ^{sca} of elastically small obstacles in a thin plate scales with $k_0^3a_c^4$. Also, as $\gamma \to 1$ and $\rho_c \to \rho_0$ (no shell, only bare object), Eq. (8) reduces to

$$\sigma^{sca} \approx \frac{\pi^2(k_0a_s)^4}{16k_0}[\rho_s - \rho_0]^2. \quad (9)$$

By enforcing $A_0 = 0$, i.e. $\sigma^{sca} \approx 0$, in Eq. (8), we can derive the quasistatic design rule for cloaking:

$$\gamma^2 = \frac{\rho_c - \rho_0}{\rho_c - \rho_s}, \quad (10)$$

which relates ρ_c, ρ_s, a_s, and a_c. It is found that, to satisfy Eq. (10), ρ_c must take negative values for $\rho_s > \rho_0$ and values larger than ρ_0 for $\rho_s < \rho_0$.

For larger objects, retardation effects become important and numerical calculations using the full 8×8 matrix in Eq. (6) are necessary to analyze the problem.

It is interesting to investigate two additional types of obstacles, namely when a "clamped" and a stress-free boundary conditions are set on the inner boundary of the system ($r = a_s$), while the same conditions of continuity of U, $\partial U/\partial r$, M_r and V_r as before are hold on the outer boundary ($r = a_c$). For the first case, we have $U = \partial U/\partial r = 0$ whereas M_r and V_r are unconstrained. The 8×8 system in Eq. (6) reduces thus to a 6×6 system (see supplementary materials[45]). Applying the analysis described before to this case reveals that the monopole scattering coefficient $A_0 \approx -1$ in the quasistatic limit regardless of the cloak's parameters. This means that the resulting scattering amplitude $f(\theta) \approx -2/\sqrt{\pi k}$ (or the scattering cross-section $\sigma^{sca} \approx 4/k$) becomes singular in the quasistatic limit (all other scattering coefficients tend to zero). This is unique to elastic waves, because a very small object would scatter infinitely and it has no equivalent in electromagnetics or acoustics[46]. This discussion shows that it is not possible to use shells of tailored density, in the quasistatic limit, to cancel the monopole scattering of a clamped obstacle since their corresponding coefficients differ by a factor $(k_0a_c)^2$.

For the stress-free boundary conditions, M_r and V_r are set to zero on $r = a_s$ whereas the same continuity conditions hold for the other parameters. We obtain here also a 6×6 system (see supplementary materials[45]). By applying the analysis above, we show that the monopole scattering coefficient of a stress-free hole of radius a_s cloaked with a shell of density ρ_c and radius $a_c = a_s/\gamma$, is given by $A_0 \approx \frac{-i\pi}{8}[1 + \gamma^2(v+1)/(v-1) + (\gamma^2 - 1)\rho_c/\rho_0]$. We see then that it is possible to find values of the density of the shell ρ_c and ratio γ that make A_0 vanish thereby canceling the scattering from the cloaked object in the quasistatic regime. This condition is found to be $\rho_c/\rho_0 = [1 + \gamma^2(v+1)/(v-1)]/(1-\gamma^2)$.

In all the results presented in the rest of the Report, in-plane dimension of the object is set to $a_s = 1$ m. Figure 2 shows the dependence of the scattering amplitude $|f(\theta)|$ on k_0a_s for $\rho_s/\rho_0 = 0.1$ [Figs. 2(a), 2(b) and 2(c)] and $\rho_s/\rho_0 = 10$ [Figs. 2(d), 2(e) and 2(f)]. We show here that curves of scattering amplitude $|f(\theta)|$ vs. θ in logarithmic scale contain angular information about the scatterer [Figs. 2(a), 2(b) and 2(d), 2(e)] and curves of normalized backward scattering amplitude $|f(\pi)|/\sqrt{a_s}$ vs. k_0a_s [Figs. 2(c) and 2(f)] give insight into the spectral dependence of the object visibility for an observer placed at the angular position of the illumination (monostatic scattering). The simulations are carried out for the first scenario (soft object e.g. soil) for $k_0a_s = 0.1$ (quasistatic limit) and $k_0a_s = 1$ (Mie scattering). It is clearly seen that, for the soft object with $\rho_s/\rho_0 = 0.1$ [Figs. 2(a) and (d)] and the rigid object with $\rho_s/\rho_0 = 10$, [Figs. 2(b) and 2(e)], the scattering amplitude $|f(\theta)|$ is circularly symmetric for $k_0a_s = 0.1$. This is due to the fact that scattering is dominated by the monopole term A_0. The scattering behavior of soft and rigid objects is quite different for different values of k_0a_s. For the soft object [Figs. 2(a), 2(b), solid red lines] A_0 is still dominant for $k_0a_s = 1$, and no significant angular dependence is observed. For the rigid object, [Figs. 2(e), solid red line], higher order multipoles start to contribute quite significantly to the overall scattering when the size is increased to $k_0a_s = 1$. This has consequences on cloaking behavior. Consider the soft and rigid objects cloaked with shells with $\rho_c = 1.3\rho_0$ and $\rho_c = -2\rho_0$, respectively. For both shells, $\gamma = 0.5$, i.e. $a_c = 2a_s$. Note that these values satisfy Eq. (10). Scattering amplitude $|f(\theta)|$ and normalized backward scattering amplitude $|f(\pi)|/\sqrt{a_s}$ of the cloaked objects are shown in Fig. 2 (dashed blue lines). Scattering reduction is clearly observed for both objects in the long wavelength limit while in the Mie scattering regime only the soft object gets cloaked in every direction.

Also, curves of $|f(\pi)|/\sqrt{a_s}$ vs. k_0a_s in Figs. 2(c) and 2(f) show that the scattering from the rigid object undergoes a more dynamic variation in k_0a_s-range [0, 1], contrary to the scattering from the soft object, where only one broad maximum is observed in the same k_0a_s-range. This is associated with the fact that higher densities correspond to smaller effective wavelengths in the object, thus causing several internal resonances even for moderately sized objects. In addition, scattering reduction is more pronounced and broader for cloaking of the soft object [Fig. 2(c) and 2(f)].

We now analyze how introducing a suitably designed negative density shell can drastically lower the overall scattering. We schematically indicate the scattering, in analogy with the polarization in the electromagnetic case, with vertical arrows of opposite direction: the positive (solid) arrow stands for 'positive' scattered wave, whereas the negative (dashed) one corresponds to scattering with opposite phase [inset of Fig. 3(b)]. Figure 3(a) shows the contours of $|\rho_c/\rho_0|$ (in logarithmic scale) that fulfill Eq. (10) for varying values of ρ_s/ρ_0 and γ. The solid blue line in the figure represents the case $\rho_c = 0$ and $+$ or $-$ sign indicates whether the required shell density is positive or negative. Let e^{sca} represent the scattering efficiency computed by the ratio of scattering cross-sections of the cloaked and bare objects. Figure 3(b) plots e^{sca} vs. ρ_c/ρ_0 for a cloaked object with $\rho_s/\rho_0 = 10$ for various values of γ and for $k_0a_s = 0.1$ (the quasistatic limit). Figure 3
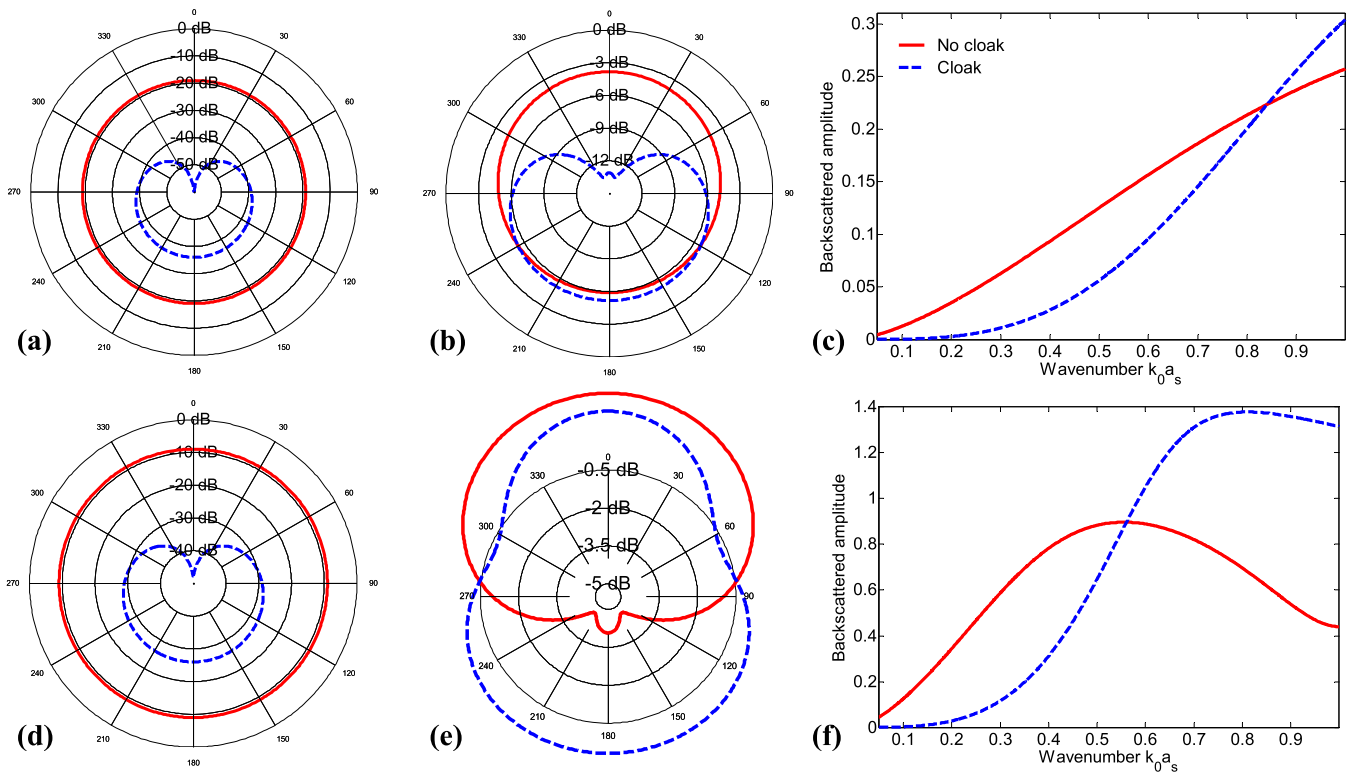
Figure 2 | Scattering amplitude $|f(\theta)|$ in logarithmic scale for the soft object ($\rho_s/\rho_0 = 0.1$) with (a) $k_0a_s = 0.1$ and (b) $k_0a_s = 1$ and for the rigid object ($\rho_s/\rho_0 = 10$) with (d) $k_0a_s = 0.1$ and (e) $k_0a_s = 1$. The dashed blue line represents the cloaked scenario whereas the solid red line stands for the bare object. Plots in (c) and (f) are the normalized backward scattering amplitude $|f(\pi)|/\sqrt{a_s}$ vs. k_0a_s for soft and rigid objects, respectively.

clearly shows that for certain values of ρ_c, significant scattering reduction is achieved, and this is also obtained for different values of γ. We notice that, for an ultrathin cloak (in the limit of $\gamma \approx 1$), there is no dip in e^{sca}; instead the scattering reduction can be quite broadband for thicker shells. For instance, the shell with $\gamma = 0.5$ and $\rho_c/\rho_0 = -2$ significantly suppresses the scattering. This agrees well with the result given by Eq. (8), which considers only the zeroth-order multipole. As schematized in the inset of Fig. 3(a), a platonic cover with relative density less than unity may induce an out-of-phase monopolar mode with respect to the local elastic displacement field, thus permitting dramatic cancellation of the field scattered from the

object. For other values of γ, different values of ρ_c/ρ_0 ranging from negative values to low positive (less than unity), are required to achieve significant cancellation of scattering.

In reality, while modeling the frequency response of the cloaking phenomenon, one needs to take into account the inherent dispersion characteristics of the shell material since it is not possible to have a negative and frequency independent density due to causality considerations[47]. A negative density metamaterial may be achieved in acoustics by mimicking the way we achieve negative permittivity in electromagnetics with low frequency homogenization in high contrast periodic media[47–52], or high frequency[53] and high order homo-
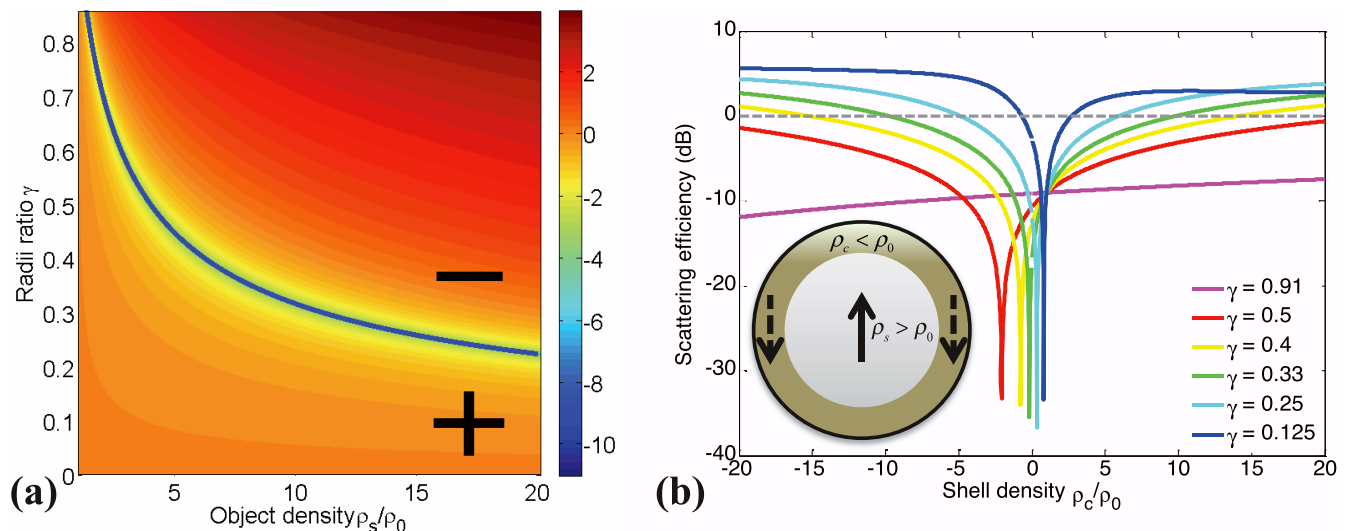

Figure 3 | (a) Contour plot of the solutions of Eq. (10). (b) Scattering efficiency e^{sca} of the cloaked object with $\rho_s/\rho_0 = 10$ vs. ρ_c/ρ_0 for various values of γ and $k_0a_s = 0.1$. The inset gives the sketch of cloaked object with arrows marking opposite phase of scattered wave in core and shell.
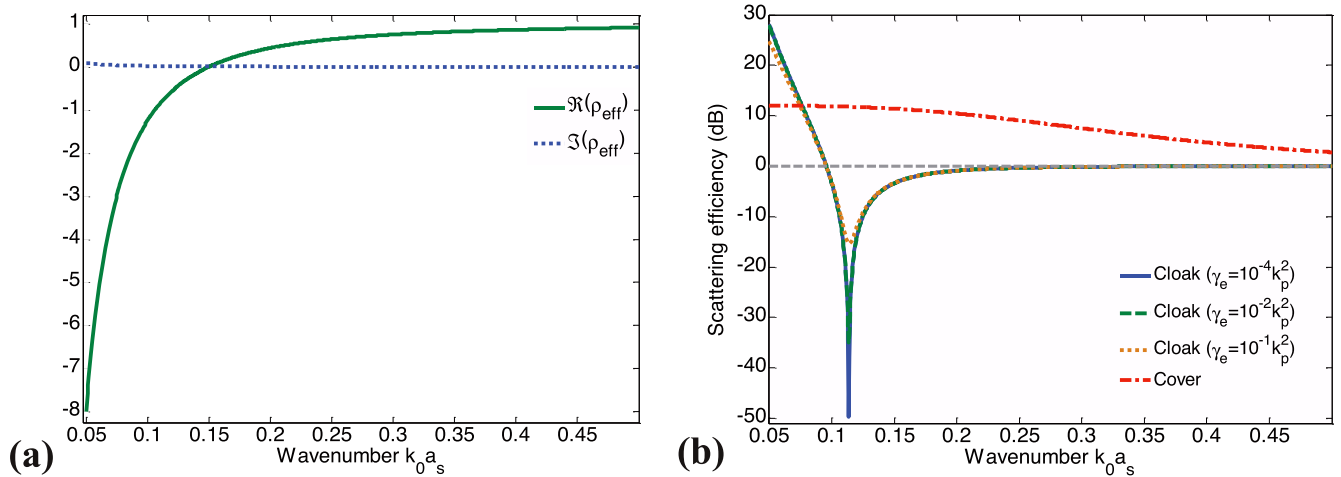
Figure 4 | (a) The *Drude-like* density dispersion of the shell material with $k_p a_s = 0.15$ and $\gamma_e = 10^{-2} k_p^2$. (b) Scattering efficiency e^{sca} of the cloaked object with $\rho_s/\rho_0 = 10$ vs. $k_0 a_s$ for various values of γ_e and $\gamma = 0.5$.

genization[54] in moderate contrast media. For elasticity, spring mass or inertial resonator metamaterials could lead to the desired effect near the resonance frequencies[55]. We suppose in the following that the material comprising the shell follows a classic *Drude-like* model of the type $\rho_c(k_0)/\rho_0 = \rho_{inf} - \dfrac{k_p^4}{k_0^2(k_0^2 + i\gamma_e)}$ [notice the fourth order dependence on k_0 stemming from the nature of the biharmonic equation], where $\rho_{inf} = 1$, and k_p and γ_e are the *plasma* wavenumber and *Ohmic* loss, respectively. This model can be obtained via a homogenization applied to a composite shell with high contrast inclusions, and is in all ways analogous to that derived in[56]. This *Drude* dispersion is plotted in Fig. 4(a) with parameters $k_p a_s = 0.15$ and $\gamma_e = 10^{-2} k_p^2$. Figure 4 (b) plots scattering efficiency e^{sca} of an object cloaked with a shell made of Drude material vs. $k_0 a_s$ for various values of γ_e. For this example, $\rho_s/\rho_0 = 10$ and $\gamma = 0.5$. Here, $\gamma_e = 10^{-4} k_p^2$, (blue solid line), $\gamma_e = 10^{-2} k_p^2$, (green dashed line), and $\gamma_e = 10^{-1} k_p^2$, (orange dotted line) correspond to small, moderate, and high Ohmic losses, respectively.

These curves are obtained using Eqs. (2) and (3), consistent with rigorous elastic scattering theory[46] and validated against results

obtained using a finite elements commercial software[57]. It is clear that the presence of a cloak with negative effective density may allow for a drastic reduction of the overall scattering at a desired wavenumber ($k_0 a_s = 0.11$ in this example), independently of the angle of observation. It is stressed here that the scattering cross-section can be reduced by over five orders of magnitude compared to the uncloaked scenario and by six orders of magnitude compared to the case of an obstacle of the same size and density $\rho_c/\rho_0 = 10$. A slight broadening of the cloaking dip and a corresponding deterioration of the effect may be noticed when elastic loss γ_e is increased.

Discussion

We have put forward a technique to cloak objects from elastic waves governed by the scalar fourth order biharmonic equation. The functionality of the obtained cloak could be seen in Fig. 5, where we plot the amplitude distribution of the scattered elastic displacement field U in the presence of cloaked [Fig. 5(a)] and uncloaked [Fig. 5(b)] objects. When it is surrounded by the negative density platonic shell (following the *Drude*-like model described above), the field amplitude is constant and equal to unity everywhere in space, in contrast to the considerably perturbed fields in the uncloaked case. The scatter-
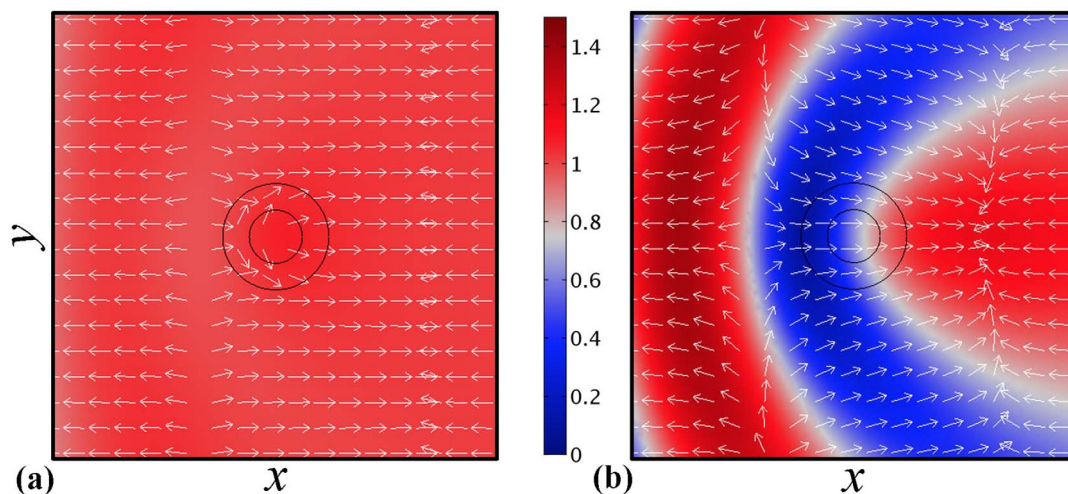

Figure 5 | **Time-averaged displacement field distributions (vector direction with white arrows, amplitude indicated by the contours) in linear scale of a rigid elastic object with $\rho_s/\rho_0 = 10$ cloaked by a *Drude*-like shell (a) and on its own for comparison (b). The structures are illuminated with a unit-amplitude plane wave ($k_0 a_s = 0.11$) propagating in the x-direction from right to left.**

ing reduction can be attributed to the proper choice of mass density of the platonic shell, in view of the scattering reduction predicted in Figs. 3 and 4.

In summary, we proposed a design of an elastic cloak based on the scattering cancellation technique, inspired by earlier applications in electrodynamics and acoustic scenarios. Here, however, the challenge is associated with the fact that a different, more complex analytical form governs bending waves. The cloaking mechanism introduced here presents significant advantages in comparison with transformation acoustic designs: there is no need of anisotropy and inhomogeneity of the material parameters. Using a homogeneous isotropic platonic shell with low or negative density we have been able to greatly reduce the scattering from soft and highly rigid objects as well as from stress-free holes. It should also be noted here that the proposed technique cannot be used to cloak clamped objects in the quasistatic limit. However, cloaks made of layered shells have the potential to overcome this problem at higher frequencies (where scattering from clamped objects is finite) by adding extra degrees of freedom to cancel more than one scattering coefficient, as previously demonstrated in electromagnetic cloak designs[58].

Experimental realization of this idea may be within reach in the near future (note for instance that lensing of bending waves via negative refraction was theoretically predicted using the biharmonic plate model in[41,42] and experimentally confirmed in a thin Duralumium plate in[59] and a theoretical proposal for cloaking via geometric transforms in the biharmonic operator was also experimentally confirmed in[37,38]), allowing for exciting applications in scenarios in which it is desirable to suppress the scattering from obstacles in thin plates in the motor vehicle and airplane industry, in which the scattering of bending waves in thin plates generated by engines may be totally suppressed, or smart secure buildings, protecting them from bending and other types of seismic vibration damages caused by scattering from neighboring buildings[60].

Methods

Analytical methods based on scattering Mie theory of cylindrical objects in thin elastic plates are used to obtain the numerical simulations in this Report (for further details and physical insight, see supplementary material[45]). The vertical displacement of the plate is the solution of the fourth order partial differential equation of Kirchhoff. We proceed, as is usually done, by expanding the impinging plane waves and the scattered fields in terms of Bessel and Hankel functions in polar coordinate system centered with the object to be cloaked. We then apply four elastodynamic boundary conditions on each cylindrical interface in order to obtain the scattering coefficients for waves, which uniquely determine the displacement fields everywhere. The displacement field distributions and scattering cross sections are computed using Bessel developments and Eq. (6) respectively. In the quasistatic limit, where the size of the elastic core sphere is much smaller than the wavelength and only the lowest-order Mie coefficient is important, an analytical formula is obtained [Eq. (10)] and it gives similar results to the full-wave simulations. Proper convergence for all the results is reached. The simulations given in Fig. 5 are obtained using the commercial finite-elements software COMSOL Multiphysics.

1. Pendry, J. B. Negative refraction makes a perfect Lens. *Phys. Rev. Lett.* **85**, 3966–3969 (2000).
2. Alù, A. & Engheta, N. Achieving transparency with plasmonic and metamaterial coatings. *Phys. Rev. E* **72**, 016623 (2005).
3. Milton, G. W. & Nicorovici, N. A. On the cloaking effects associated with anomalous localized resonance. *Proc. Roy. Lond. A* **462**, 3027–3059 (2006).
4. Mühlig, S., Farhat, M., Rockstuhl, C. & Lederer, F. Cloaking dielectric spherical objects by a shell of metallic nanoparticles. *Phys. Rev. B* **83**, 195116 (2011).
5. Farhat, M., Mühlig, S., Rockstuhl, C. & Lederer, F. Scattering cancellation of the magnetic dipole field from macroscopic spheres. *Opt. Express* **20**, 13896–13906 (2012).
6. Farhat, M., Rockstuhl, C. & Bagci, H. A 3D tunable and multi-frequency graphene plasmonic cloak. *Opt. Express* **21**, 12592–12603 (2013).
7. Xi, S., Chen, H., Zhang, B., Wu, B. I. & Kong, J. A. Route to low-scattering cylindrical cloaks with finite permittivity and permeability. *Phys. Rev. B* **79**, 155122 (2009).
8. Alù, A. & Engheta, N. Plasmonic materials in transparency and cloaking problems: mechanism, robustness, and physical insights. *Opt. Express* **15**, 3318–3332 (2007).
9. Chen, P.-Y., Soric, J. & Alù, A. Invisibility and cloaking based on scattering cancellation. *Adv. Mater.* **24**, 281–304 (2012).
10. Malureanu, R. *et al.* A new method for obtaining transparent electrodes. *Opt. Express* **20**, 22770–22782 (2012).
11. Song, Z., He, Q., Xiao, S. & Zhou, L. Making a continuous metal film transparent via scattering cancellations. *Appl. Phys. Lett.* **101**, 181110 (2012).
12. Edwards, B., Alù, A., Silveirinha, M. G. & Engheta, N. Experimental verification of plasmonic cloaking at microwave frequencies with metamaterials. *Phys. Rev. Lett.* **103**, 153901 (2009).
13. Rainwater, D. *et al.* Experimental verification of three-dimensional plasmonic cloaking in free-space. *New J. Phys.* **14**, 013054 (2012).
14. Xu, S. *et al.* Experimental Demonstration of a Free-Space Cylindrical Cloak without Superluminal Propagation. *Phys. Rev. Lett.* **109**, 223903 (2012).
15. Pendry, J. B., Schurig, D. & Smith, D. R. Controlling electromagnetic fields. *Science* **312**, 1780 (2006).
16. Leonhardt, U. Optical conformal mapping. *Science* **312**, 1777–1780 (2006).
17. Schurig, D. *et al.* Metamaterial electromagnetic cloak at microwave frequencies. *Science* **314**, 977–980 (2006).
18. Cai, W., Chettiar, U. K., Kildiev, A. V. & Shalaev, V. M. Optical cloaking with metamaterials. *Nat. Photonics* **1**, 224–227 (2007).
19. Smolyaninov, I. I., Smolyaninova, V. N., Kildishev, A. V. & Shalaev, V. M. Anisotropic metamaterials emulated by tapered waveguides: application to optical cloaking. *Phys. Rev. Lett.* **102**, 213901 (2009).
20. Valentine, J., Li, J., Zentgraf, T., Bartal, G. & Zhang, X. An optical cloak made of dielectrics. *Nat. Mater.* **8**, 568–571 (2009).
21. Ergin, T., Stenger, N., Brenner, P., Pendry, J. B. & Wegener, M. Three-dimensional invisibility cloak at optical wavelengths. *Science* **328**, 337–339 (2010).
22. Zhang, B. Electrodynamics of transformation-based invisibility cloaking. *Light: Science & Applications* **1**, 32 (2012).
23. Alù, A. & Engheta, N. Cloaking a sensor. *Phys. Rev. Lett.* **102**, 233901 (2009).
24. Alù, A. & Engheta, N. Cloaked near-field scanning optical microscope tip for noninvasive near-field imaging. *Phys. Rev. Lett.* **105**, 263906 (2010).
25. Cummer, S. A. & Schurig, D. One path to acoustic cloaking. *New J. Phys.* **9**, 45 (2007).
26. Torrent, D. & Sanchez-Dehesa, J. Acoustic cloaking in two dimensions: a feasible approach. *New J. Phys.* **10**, 063015 (2008).
27. Farhat, M., Enoch, S., Guenneau, S. & Movchan, A. B. Broadband cylindrical acoustic cloak for linear surface waves in a fluid. *Phys. Rev. Lett.* **101**, 134501 (2008).
28. Chen, H. & Chan, C. T. Acoustic cloaking in three dimensions using acoustic metamaterials. *Appl. Phys. Lett.* **91**, 183518 (2007).
29. Cummer, S. A. *et al.* Scattering theory derivation of a 3D acoustic cloaking shell. *Phys. Rev. Lett.* **100**, 024301 (2008).
30. Guild, M. D., Haberman, M. R. & Alù, A. Plasmonic-type acoustic cloak made of a bilaminate shell. *Phys. Rev. B* **86**, 104302 (2012).
31. Guild, M. D., Haberman, M. R. & Alù, A. Plasmonic cloaking and scattering cancelation for electromagnetic and acoustic waves. *Wave Motion* **48**, 468–482 (2011).
32. Guild, M. D., Alù, A. & Haberman, M. R. Cancellation of acoustic scattering from an elastic sphere. *J. Acoust. Soc. Am.* **129**, 1355–1365 (2011).
33. Milton, G. W., Briane, M. & Willis, J. R. On cloaking for elasticity and physical equations with a transformation invariant form. *New J. Phys.* **8**, 248 (2006).
34. Brun, M., Guenneau, S. & Movchan, A. B. Achieving control of in-plane elastic waves. *Appl. Phys. Lett.* **94**, 061903 (2009).
35. Farhat, M., Guenneau, S., Enoch, S. & Movchan, A. B. Cloaking bending waves propagating in thin elastic plates. *Phys. Rev. B* **79**, 033102 (2009).
36. Norris, A. N. Acoustic metafluids. *J. Acoust. Soc. Am.* **125**, 839–849 (2009).
37. Farhat, M., Guenneau, S. & Enoch, S. Ultrabroadband elastic cloaking in thin plates. *Phys. Rev. Lett.* **103**, 024301 (2009).
38. Stenger, N., Wilhelm, M. & Wegener, M. Experiments on elastic cloaking in thin plates. *Phys. Rev. Lett.* **108**, 014301 (2012).
39. Timoshenko, S. *Theory of Plates and Shells* (McGraw-Hill, New York, 1940).
40. Graff, K. F. *Wave Motion in Elastic Solids* (Dover, New York, 1975).
41. Farhat, M., Guenneau, S., Enoch, S., Movchan, A. B. & Petursson, G. G. Focussing bending waves via negative refraction in perforated thin plates. *Appl. Phys. Lett.* **96**, 081909 (2010).
42. Farhat, M., Guenneau, S. & Enoch, S. High directivity and confinement of flexural waves through ultra-refraction in thin perforated plates. *EPL-Europhys. Lett.* **91**, 54003 (2010).
43. Movchan, N. V., McPhedran, R. C., Movchan, A. B. & Poulton, C. G. Wave scattering by platonic grating stacks. *Proc. R. Soc. A-Math. Phys. Eng. Sci.* **465**, 3383–3400 (2009).
44. Antonakakis, T. & Craster, R. V. High-frequency asymptotics for microstructured thin elastic plates and platonics. *Proc. R. Soc. Lond. A-Math. Phys. Eng. Sci.* **468**, 1408–1427 (2012).
45. Supplemental materials section.
46. Norris, A. N. & Vemula, C. Scattering of flexural waves on thin plates. *J. Sound Vibr.* **181**, 115–125 (1995).
47. Mei, J., Ma, G., Yang, M., Yang, J. & Sheng, P. [Dynamic Mass Density and Acoustic Metamaterials] *Acoustic Metamaterials and Phononic Crystals* [Deymier, P. A. (ed.)] [159–200] (Springer-Verlag, Berlin, 2013).
48. Li, J. & Chan, C. T. Double-negative acoustic metamaterial. *Phys. Rev. E* **70**, 055602(R) (2004).

49. Liu, Z., Chan, C. T. & Sheng, P. Analytic model of phononic crystals with local resonances. *Phys. Rev. B* **71**, 014103 (2005).
50. Mei, J., Liu, Z., Wen, W. & Sheng, P. Effective dynamic mass density of composites. *Phys. Rev. B* **76**, 134205 (2007).
51. Wu, Y., Lai, Y. & Zhang, Z. Q. Elastic metamaterials with simultaneously negative effective shear modulus and mass density. *Phys. Rev. Lett.* **107**, 105506 (2011).
52. Zhou, X., Liu, X. & Hu, G. Elastic metamaterials with local resonances: an overview. *Theor. Appl. Mech. Lett.* **2**, 041001 (2012).
53. Craster, R. V., Kaplunov, K. & Pichugin, A. V. High-frequency homogenization for periodic media. *Proc. R. Soc. A-Math. Phys. Eng. Sci.* **466**, 2341–2362 (2010).
54. Liu, Y., Guenneau, S. & Gralak, B. Causality and passivity properties of effective parameters of electromagnetic multilayered structures. *Proc. R. Soc. A-Math. Phys. Eng. Sci.* **469**, 20130240 (2013).
55. Bigoni, D., Guenneau, S., Movchan, A. B. & Brun, M. Elastic metamaterials with inertial locally resonant structures: Application to lensing and localization. *Phys. Rev. B* **87**, 174303 (2013).
56. Farhat, M., Chen, P. Y., Guenneau, S., Enoch, S. & Alù, A. Frequency-selective surface acoustic invisibility for three-dimensional immersed objects. *Phys. Rev. B* **86**, 174303 (2012).
57. COMSOL Multiphysics, http://www.comsol.com (2014).
58. Alù, A. & Engheta, N. Plasmonic and metamaterial cloaking: physical mechanisms and potentials. *J. Opt.* **10**, 093002 (2008).
59. Dubois, M. *et al.* Flat lens for pulse focusing of elastic waves in thin plates. *Appl. Phys. Lett.* **103**, 071915 (2013).
60. Brulé, S., Javelaud, E., Enoch, S. & Guenneau, S. Seismic metamaterial: how to shake friends and influence waves? arXiv:1301.7642 (2012).

Author contributions

M.F., P.-Y.C. and A.A. conceived the theoretical idea. M.F. conducted the numerical simulations and wrote the manuscript text. P.-Y.C., H.B., S.E., S.G. and A.A. discussed the implementation of the concept and reviewed the manuscript.

Additional information

Supplementary information accompanies this paper at http://www.nature.com/scientificreports

Competing financial interests: The authors declare no competing financial interests.

How to cite this article: Farhat, M. *et al.* Platonic Scattering Cancellation for Bending Waves in a Thin Plate. *Sci. Rep.* **4**, 4644; DOI:10.1038/srep04644 (2014).